Influence of Electrical Eigenfrequencies on Damped Voltage Resonance Based Sensorless Control of Switched Reluctance Drives

K.R. Geldhof, A. Van den Bossche and J.A.A. Melkebeek

Department of Electrical Energy, Systems and Automation (EESA)
Ghent University (UGent), Sint-Pietersnieuwstraat 41, B-9000 Gent, Belgium
phone: +32 (0)9 264 3442, fax: +32 (0)9 264 3582
e-mail: Kristof.Geldhof@UGent.be

***Abstract*—In switched reluctance motor drives, the combination of power-electronic converter and a motor phase defines a resonant circuit, comprised by the motor phase inductance and the parasitic capacitance of converter switches, power cables and motor phase winding. If a motor phase is excited by applying very short voltage pulses, the resonance frequency of the circuit can be observed through the subsequent damped oscillation of the induced voltage in the phase. As the phase inductance and associated resonance frequency depend on the rotor position, the method provides a means for estimating the rotor position.**

This paper discusses the influence of the magnetic inductive coupling between motor phases on the observed damped voltage resonance. It is shown that the motor-converter combination can be modelled as a system comprising different resonant circuits, each associated with one phase of the machine, which are mutually coupled due to the inductive coupling between the motor phases. An eigenvalue analysis reveals the different eigenfrequencies and modes of oscillation for this system. It follows from the analysis that damped voltage resonances occur in all phases of the machine due to the mutual coupling. The model is used to determine the influence of voltage pulses, applied to a single phase or simultaneously applied to different phases, on the observed damped voltage oscillations, and thus on the rotor position estimation.

I. Introduction

Position- or speed-sensorless control of switched reluctance machines receives a lot of interest from the industrial and academic community.

One class of sensorless methods for switched reluctance motors is based on the excitation of a series resonant circuit comprised by the position-dependent inductance of an idle motor phase, an external capacitor and a resistor [1]. If a high-frequency sinusoidal current is injected in the circuit, the amplitude and phase of a voltage in the circuit is modulated by the rotor position.

A rotor position estimation method based on electrical resonance, but without the need for an external excitation circuit, is proposed in [2] [3]. The method is characterized by the fact that very short voltage pulses are used to trigger resonance between the magnetic energy stored in the phase inductances and the energy stored in parasitic capacitances associated with the power semiconductor devices, power cables and motor phase windings.

In this paper, the influence of magnetic inductive coupling between the phases is discussed with regard to [2]. Inductive coupling has previously been used to detect rotor position, through the measurement of induced voltages [4]. With regard to [2], it is shown that the combination of motor and converter can be modelled by means of a number of resonant circuits which are mutually coupled due to the magnetic inductive coupling between motor phases. By means of an eigenmode analysis, the influence of voltage pulses, applied to a single phase or simultaneously applied to different phases, on the initiated resonances, and thus on the rotor position estimation, is studied.

II. Damped voltage resonance

Fig. 1 shows a configuration comprising an asymmetric H-bridge of a switched reluctance drive converter (using IGBTs as switching devices) and a motor phase. It is assumed here that the IGBTs and freewheeling diodes are blocked, which means that the behaviour of these devices is mainly determined by a parasitic capacitance. The physical origin of this capacitance lies in the depletion layer, which is essentially an isolating layer between the conducting doped regions of the semiconductor devices. The capacitances C_i and C_d for the IGBTs and diodes respectively are indicated in the parasitic model of Fig. 2. This model also shows the bus bar capacitance C_b, the capacitance C_c of the power cable between H-bridge and motor phase, and the parasitic capacitance C_w of the motor phase winding. The latter is a discrete equivalent for the distributed inter-turn capacitances of the winding. The impedance $\underline{Z}_\mathrm{w}$ represents the phase winding impedance without the contribution of the parasitic capacitance C_w.

We will assume here that the parasitic capacitances C_i and C_d of the semiconductor devices are constant. This is a strong simplification, as both capacitances show a strong nonlinear dependence on the voltage across them. With the constant capacitance assumption, and taking into account that $C_\mathrm{i}, C_\mathrm{d} \ll C_\mathrm{b}$, the combined motor-converter circuit reduces to

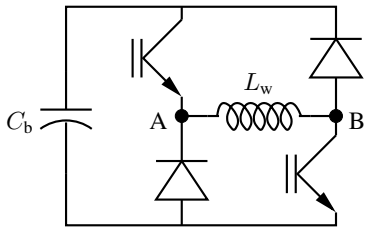

Fig. 1. Converter H-bridge and phase winding of a switched reluctance drive

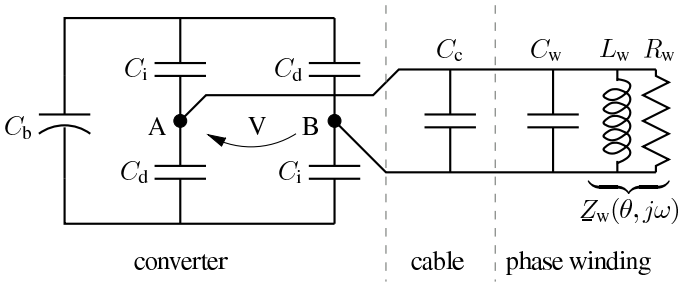

Fig. 2. Parasitic model for the combination of a motor phase and converter H-bridge

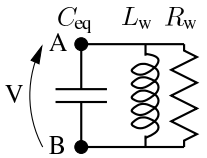

Fig. 3. Equivalent resonant LRC circuit

the equivalent parallel LRC circuit of Fig. 3, with an equivalent capacitance C_{eq} given by

$$C_{\text{eq}} = \frac{C_{\text{i}} + C_{\text{d}}}{2} + C_{\text{c}} + C_{\text{w}}. \tag{1}$$

The circuit of Fig. 3 has an undamped resonance frequency ω_{res} given by

$$\omega_{\text{res}} = \frac{1}{\sqrt{L_{\text{w}}(\theta, \omega_{\text{res}}) C_{\text{eq}}}}. \tag{2}$$

As can be seen from (2), ω_{res} depends on the rotor position. The undamped resonance frequency will reach a maximum value for the unaligned rotor position (minimum phase inductance) and a minimum value for the aligned rotor position (maximum phase inductance).

In order to observe this resonance frequency, a very short voltage pulse can be applied to the motor phase [2]. This has the effect that the parasitic phase winding capacitance C_{w} (and also the cable capacitance C_{c} and diode capacitance C_{d}) is charged up to the DC bus voltage V_{dc}, and that the initial voltage distribution of Fig. 4 is realized. After the application of the short voltage pulse, the circuit is let to oscillate freely. Thereby, an energy exchange occurs between the capacitive and inductive elements in the circuit of Fig. 2. The associated resonance can be clearly observed in the phase voltage. Fig. 5 shows an example of a 1.2 μs voltage test pulse applied to the phase winding, and the resonances initiated by the test pulse

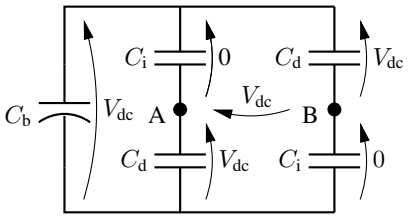

Fig. 4. Initial energy distribution after short voltage pulse

when the rotor is aligned or unaligned with respect to the test phase. The resonances are damped due to eddy current and hysteresis loss in the magnetic core of the machine [5]. The damping is stronger in the aligned rotor position as the iron path dominates the air gap in the magnetic path.

The difference in resonance between the aligned and unaligned rotor position can be used to obtain position information [2]. One possibility is to measure the resonating voltage at a fixed time t_s relative to the start of the voltage test pulse, as shown in Fig. 5. This voltage sample can be mapped to the rotor position at which the sample was measured. Fig. 6 shows the mapping between different rotor positions and the associated voltage samples. Fig. 6 provides a position signature of the SRM drive. The data of Fig. 6 can be stored in a look-up table, the input of which is the measured voltage sample and the output of which is the rotor position. Different position signatures can be established if the parameter t_s is varied. The time t_s is preferably chosen to be close to one half of the unaligned resonance period. This results in a good position resolution due to the large difference between unaligned and aligned voltage samples.

The measured resonances of Fig. 5(b) were obtained by applying short voltage pulses in phase A of a 3-phase 6x4 machine, while the remaining phases B and C were disconnected from the converter. Therefore, the (undamped) resonance frequency of the oscillating voltage in phase A is determined by the phase inductance L_a and the total parasitic capacitance C_{eq} associated with phase A.

However, if phases B and C are connected to the converter, the combination of each phase winding and the parasitic capacitance of its associated converter bridge defines an additional resonant circuit. Moreover, the three resonant circuits are mutually coupled due to the magnetic inductive coupling between the motor phases. The resulting system, with omitted damping resistors, is schematically shown in Fig. 7. It must be noted that this model is only valid under the assumption that the IGBTs and diodes of phase B and C are not conducting, so that these devices behave as a parasitic capacitance. This is the case when the switched reluctance motor is unloaded. In the following section, an eigenmode analysis is done on the coupled system to calculate the phase voltage oscillation after application of a short voltage pulse.

III. No-load eigenmode analysis

In the case of an unloaded motor, the motor-converter combination can be modelled by a system with 3 degrees

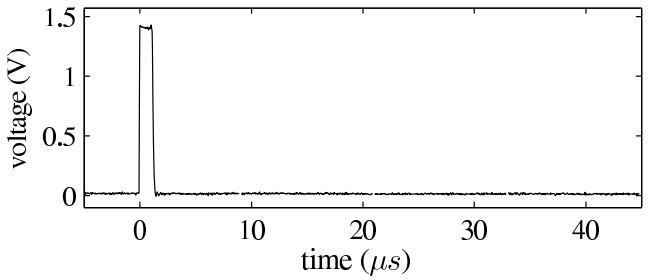

(a) Control signal for IGBTs (signal before gate drive circuit).

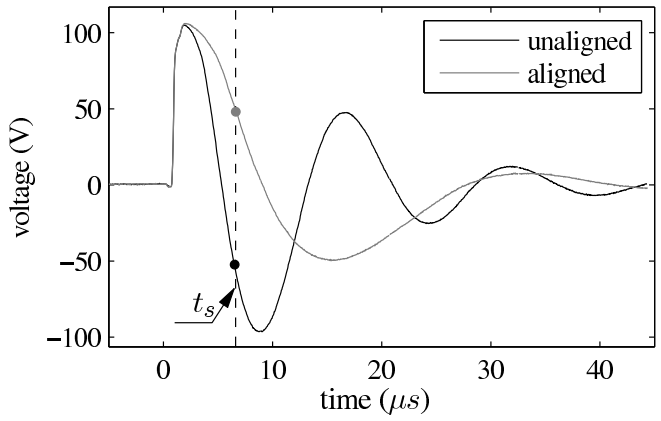

(b) Phase voltage

Fig. 5. Measured resonance after application of a 1.2 μs voltage pulse in phase A. Phases B and C were disconnected from the converter. DC bus bar voltage $V_{\text{dc}} = 105\ V$. Motor at standstill. Aligned resonance frequency: 32.9 kHz. Unaligned resonance frequency: 64.9 kHz.

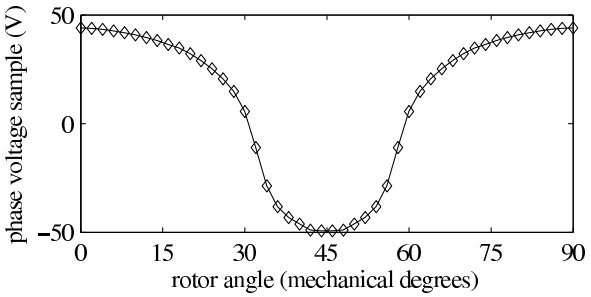

Fig. 6. Measured position signature for the 6x4 switched reluctance motor. The aligned rotor position corresponds to 0°, the unaligned position corresponds to 45°.

of freedom, see Fig. 7. This system shows analogy with a mechanical spring-mass system where three masses can oscillate [6]. An eigenmode analysis can be done on this system. For this purpose, some assumptions are made.

- It is assumed that the parasitic capacitance associated with each phase is constant, and that it has the same value for each phase. In reality, the parasitic capacitance of the power semiconductor devices (which is the dominant capacitance in C_{eq}) is strongly voltage-dependent. Fig. 8 shows the measured voltage dependence of the drain-source capacitance of an IGBT in a Fairchild FCASN50SN60 smart power module used in the experimental set-up. The capacitance shows a sharp drop if the voltage is increased from zero, but the decrease is much less for voltages above 20 V, i.e. when the phase voltage drops below 60 V. It can be seen from Fig. 5(b) that the phase voltage has already dropped below this value before the time instant t_s. In a significant part of the time frame in which the resonance occurs, the equivalent capacitance C_{eq} remains almost constant, which justifies the assumption.
- It is assumed that the system is undamped. In reality, the damping induced by eddy currents in the laminations of the machine leads to a frequency-dependence of the self and mutual inductances. It is assumed that each inductance has the same value at the different eigenfrequencies of the system. This assumption can be justified by the fact that air gaps in the self and mutual magnetic paths of the machine reduce the frequency-dependence of the inductances.
- Low speed is assumed, so that voltage contributions due to electromotive force can be neglected.
- Resistive voltage drop in the phase windings is neglected.

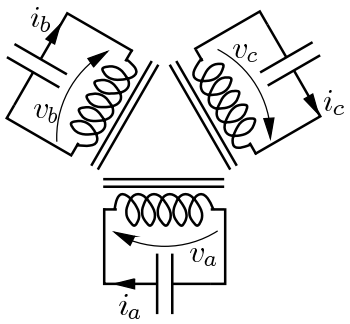

Fig. 7. Model of magnetically coupled resonant circuits for the unloaded 3-phase switched reluctance drive.

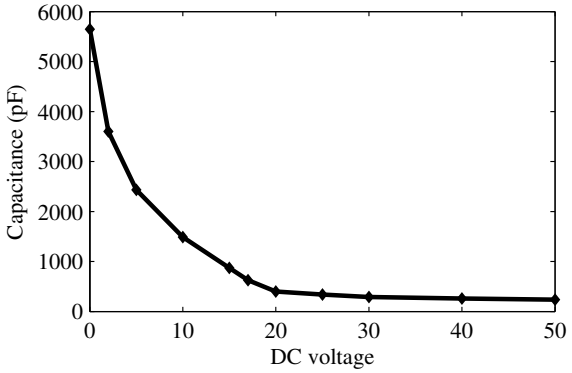

Fig. 8. Measured voltage-dependence of IGBT drain-source capacitance.

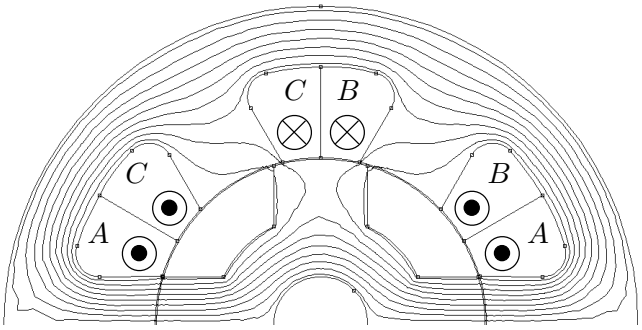

Fig. 9. Geometry (one half) of the 6x4 switched reluctance motor, with indication of current references. Flux lines are shown for a harmonic calculation at 32.9 kHz with phase A excited.

With these assumptions, the phase voltage equations in a harmonic regime at frequency ω are given by

$$V_a = j\omega(L_a I_a + M_{ab} I_b + M_{ac} I_c) \quad (3)$$
$$V_b = j\omega(M_{ab} I_a + L_b I_b + M_{bc} I_c) \quad (4)$$
$$V_c = j\omega(M_{ac} I_a + M_{bc} I_b + L_c I_c), \quad (5)$$

where V_a, V_b, V_c are the phase voltage phasors, I_a, I_b, I_c the phase current phasors, L_a, L_b, L_c the phase self inductances and M_{ab}, M_{ac}, M_{bc} the mutual inductances between each pair of phases. Furthermore, each phase is loaded with a parasitic capacitance C_{eq}:

$$I_a = -j\omega C_{\text{eq}} V_a \quad (6)$$
$$I_b = -j\omega C_{\text{eq}} V_b \quad (7)$$
$$I_c = -j\omega C_{\text{eq}} V_c. \quad (8)$$

Combination of (3–8) leads to a set of equations for the phase voltages:

$$-\omega^2 C_{\text{eq}} \underbrace{\begin{bmatrix} L_a & M_{ab} & M_{ac} \\ M_{ab} & L_b & M_{bc} \\ M_{ac} & M_{bc} & L_c \end{bmatrix}}_{\boldsymbol{L}} \begin{bmatrix} V_a \\ V_b \\ V_c \end{bmatrix} + \underbrace{\begin{bmatrix} 1 & 0 & 0 \\ 0 & 1 & 0 \\ 0 & 0 & 1 \end{bmatrix}}_{\boldsymbol{I}} \begin{bmatrix} V_a \\ V_b \\ V_c \end{bmatrix} = \begin{bmatrix} 0 \\ 0 \\ 0 \end{bmatrix} \quad (9)$$

Non-zero solutions for (9) exist if

$$\det\left(\boldsymbol{L} - \frac{1}{C_{\text{eq}}\omega^2}\boldsymbol{I}\right) = 0, \quad (10)$$

where $\boldsymbol{L}$ is the matrix with self and mutual inductances, and $\boldsymbol{I}$ is the identity matrix. Three possible values ω_i ($i = 1, 2, 3$) result from the solution of (10), corresponding to the eigenfrequencies of the system. It should be noted that the eigenfrequencies are related to the eigenvalues λ_i of the inductance matrix $\boldsymbol{L}$:

$$\lambda_i = \frac{1}{C_{\text{eq}}\omega_i^2} \quad (11)$$

Each eigenfrequency ω_i is associated with an eigenvector $\boldsymbol{V}_i$. Each eigenvector describes a way in which the degrees of freedom of the system oscillate, at the associated eigenfrequency.

The eigenfrequencies and eigenvectors were calculated for a 6x4 switched reluctance motor, with the rotor position aligned with phase A, as shown in Fig. 9. A harmonic finite element analysis was done at frequency $f = 32.9$ kHz. This corresponds to the measured resonance frequency in the aligned rotor position, see Fig. 5(b). The calculated inductance matrix $\boldsymbol{L}$ is obtained from the finite element post-processing:

$$\begin{bmatrix} L_a & M_{ab} & M_{ac} \\ M_{ab} & L_b & M_{bc} \\ M_{ac} & M_{bc} & L_c \end{bmatrix} = \begin{bmatrix} 39.65 & 4.63 & 4.63 \\ 4.63 & 22.37 & 3.82 \\ 4.63 & 3.82 & 22.36 \end{bmatrix} \text{ mH}. \quad (12)$$

With the choice of phase current references as shown in Fig. 9, the mutual inductance values in (12) are positive. If the phase winding configuration is such that the physical current flow corresponds with the current references indicated in Fig. 9, the mutual fluxes contribute to torque production. This winding configuration yields the highest output torque of the machine [7] [8].

The measurement of Fig. 5(b) shows an aligned voltage resonance of 32.9 kHz in the case of a test pulse applied to phase A, with phase B and C not connected to the converter. At this frequency, the inductance of phase A was calculated to be 39.65 mH, see (12). With these values, an estimation for the equivalent capacitance C_{eq} in (11) can be made:

$$f_{\text{res}} = \frac{1}{2\pi\sqrt{L_a C_{\text{eq}}}} = 32.9 \text{ kHz}, \quad (13)$$

which results in

$$C_{\text{eq}} = 590 \text{ pF}. \quad (14)$$

The eigenvalues and (normed) eigenvectors of (12) are listed in Table I. The table also lists the eigenfrequencies, which are calculated by means of (11).

For a given eigenmode, each phase voltage will oscillate at the eigenfrequency associated with this mode. The relative amplitude at which each phase voltage oscillates is given by the components of the eigenvector. This implies that a single eigenmode is excited only if the initial phase voltages are proportional to the eigenvector components associated with this mode. Fig. 10 shows the calculated second eigenmode of the coupled system.

In the case when a single phase is excited by means of a short test pulse, the initial voltage vector is given by

$$\boldsymbol{v}(t=0) = \begin{bmatrix} v_a(t=0) \\ v_b(t=0) \\ v_c(t=0) \end{bmatrix} = \begin{bmatrix} V_{\text{dc}} \\ 0 \\ 0 \end{bmatrix}. \quad (15)$$

As the initial voltage vector (15) is not proportional to any of the eigenvectors, the time response of each phase voltage will

TABLE I
EIGENMODES OF THE SWITCHED RELUCTANCE DRIVE FOR AN ALIGNED ROTOR POSITION.

quantity	symbol & unit	1	2	3
eigenvalue	λ_i (mH)	18.55	23.52	42.31
eigenfrequency	ω_i (kHz)	48.1	42.7	31.9
eigenvector	$\boldsymbol{V}_i$ (V)	$\begin{bmatrix} 0 \\ 0.71 \\ -0.71 \end{bmatrix}$	$\begin{bmatrix} 0.38 \\ -0.65 \\ -0.65 \end{bmatrix}$	$\begin{bmatrix} -0.92 \\ -0.26 \\ -0.26 \end{bmatrix}$

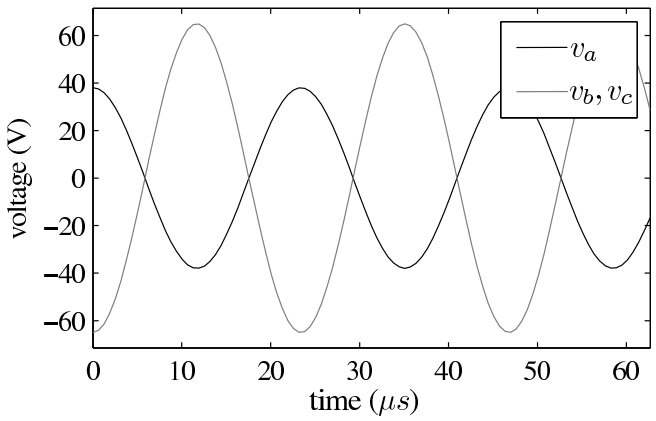

Fig. 10. Calculated phase voltages for second eigenmode: eigenfrequency 42.7 kHz, normed eigenvector [0.38 -0.65 -0.65]$^{\mathrm{T}}$.

be determined by a superposition of eigenmodes. To calculate the time response of the phases, we define a linear transformation of the phase voltages v_a, v_b, v_c to a set of *virtual* phase voltages η_a, η_b, η_c. For this purpose a transformation matrix $\boldsymbol{S}$ is constructed, the columns of which contain the eigenvectors:

$$\boldsymbol{\eta} = \boldsymbol{S}^{-1}\boldsymbol{v}, \quad \boldsymbol{S} = [\boldsymbol{V}_1; \boldsymbol{V}_2; \boldsymbol{V}_3] \tag{16}$$

Using the transformation matrix $\boldsymbol{S}$, (9) can be transformed:

$$-\omega^2 C_{\mathrm{eq}} \boldsymbol{L}\boldsymbol{S}\boldsymbol{\eta} + \boldsymbol{S}\boldsymbol{\eta} = \boldsymbol{0}. \tag{17}$$

Left-multiplication of (17) with $\boldsymbol{S}^{-1}$ results in

$$-\omega^2 C_{\mathrm{eq}} \boldsymbol{S}^{-1}\boldsymbol{L}\boldsymbol{S}\boldsymbol{\eta} + \boldsymbol{\eta} = \boldsymbol{0}. \tag{18}$$

The matrix $\boldsymbol{S}^{-1}\boldsymbol{L}\boldsymbol{S} = \boldsymbol{\lambda}$ is a diagonal matrix containing the eigenvalues λ_i of the inductance matrix $\boldsymbol{L}$:

$$-\omega^2 C_{\mathrm{eq}} \boldsymbol{\lambda}\boldsymbol{\eta} + \boldsymbol{\eta} = \boldsymbol{0}. \tag{19}$$

Equation (19) shows that the virtual system has the same eigenvalues as the original system, but orthogonal eigenvectors η_i:

$$\boldsymbol{\eta}_1 = \begin{bmatrix} 1 \\ 0 \\ 0 \end{bmatrix}, \quad \boldsymbol{\eta}_2 = \begin{bmatrix} 0 \\ 1 \\ 0 \end{bmatrix}, \quad \boldsymbol{\eta}_3 = \begin{bmatrix} 0 \\ 0 \\ 1 \end{bmatrix}, \tag{20}$$

We can now find the phase A voltage response to an initial excitation (15) by performing following steps.

1) The excitation vector (15) is transformed to an excitation vector in the virtual system. For $V_{\mathrm{dc}} = 100$ V this gives

$$\boldsymbol{\eta}(t=0) = \boldsymbol{S}^{-1} \begin{bmatrix} V_{\mathrm{dc}} \\ 0 \\ 0 \end{bmatrix} = \begin{bmatrix} 0 \\ 37.6 \\ -92.7 \end{bmatrix}. \tag{21}$$

2) Due to the orthogonality of the eigenmodes in the virtual system, the virtual voltage response is given by

$$\boldsymbol{\eta}(t) = \begin{bmatrix} 0 \\ 37.6\cos(\omega_2 t) \\ -92.7\cos(\omega_3 t) \end{bmatrix}. \tag{22}$$

3) The virtual voltages are transformed back to the original phase voltages:

$$\boldsymbol{v}(t) = \boldsymbol{S}\boldsymbol{\eta}(t) \tag{23}$$

or

$$\begin{bmatrix} v_a(t) \\ v_b(t) \\ v_c(t) \end{bmatrix} = \begin{bmatrix} 0 & 14.15 & 85.85 \\ 0.03 & -24.68 & 24.65 \\ -0.03 & -24.62 & 24.64 \end{bmatrix} \begin{bmatrix} \cos(\omega_1 t) \\ \cos(\omega_2 t) \\ \cos(\omega_3 t) \end{bmatrix}. \tag{24}$$

The phase voltage waveforms $v_a(t)$ and $v_b(t)$ are indicated by traces 2 and 3 in Fig. 11(a) and Fig. 11(b); Fig. 11(a) shows a few periods of the waveforms, while Fig. 11(b) details the first 40 μs of the waveforms. Several conclusions can be drawn from these figures.

Comparison of traces 1 and 2 shows that the inductive coupling between the phases influences the phase voltage response to a test pulse applied in that phase. It can be seen from (24) that, if mutual coupling is taken into account (trace 2), the waveform of v_a is dominated by the 3$^{\mathrm{rd}}$ eigenmode. The associated eigenfrequency 31.9 kHz is lower than the frequency 32.9 kHz in the abscence of mutual coupling. This can be explained by the fact that, in the case of inductive coupling, the mutual magnetic flux paths give rise to an equivalent higher A inductance, and hence a lower resonance frequency.

If the voltage resonance method is used for rotor position estimation, an initial position signature as in Fig. 6 has to be established. This signature can be obtained by measuring voltage samples at time t_s (as indicated in Fig. 5(b)) for subsequent rotor positions. The result of the eigenmode analysis shows the importance of measuring the position signature with all phases connected to the converter, as this corresponds to the situation during normal operation of the drive. A signature recorded with only phase A connected to the converter results in a position signature different from the signature with all phases connected, and will result in position errors during the operation of the drive.

The eigenmode analysis further shows that, even though one phase (v_a) is excited by a short voltage pulse, resonance waveforms are initiated in other motor phases (v_b and v_c). Therefore, in principle, each one of the phase voltages could be used to extract rotor position information.

IV. Application of Simultaneous Test Pulses

In the previous section, it was discussed that the motor-converter combination can be modelled by a system of three mutually coupled resonant circuits, described by (9) and schematically shown in Fig. 7. This system has three eigenmodes, which can be calculated from the inductance matrix (12). Each eigenmode resonates at an eigenfrequency, determined by (11). In the case that one of the phases is excited by a short voltage pulse, the oscillating waveforms initiated by this pulse in all motor phases are constituted by a linear combination of the eigenmodes of the system. The exact weight of each eigenmode is determined by the initial phase voltages and their time-derivatives.

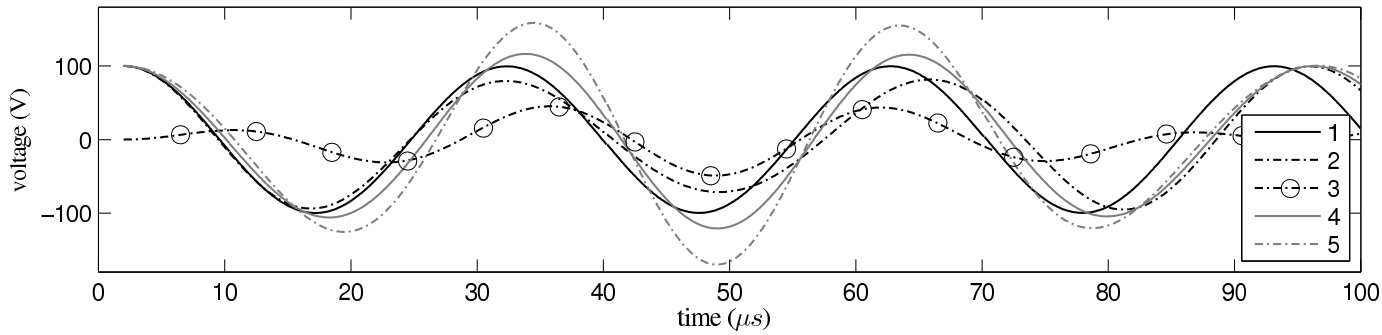

(a) Calculated waveforms

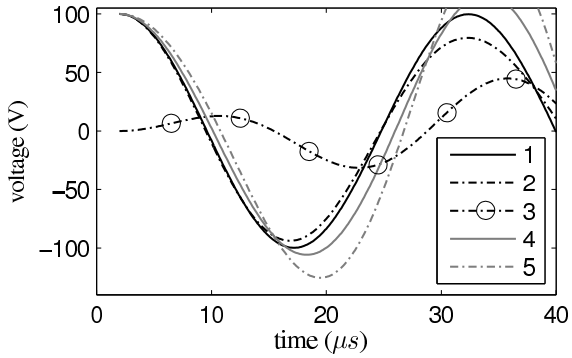

(b) Calculated waveforms - detail

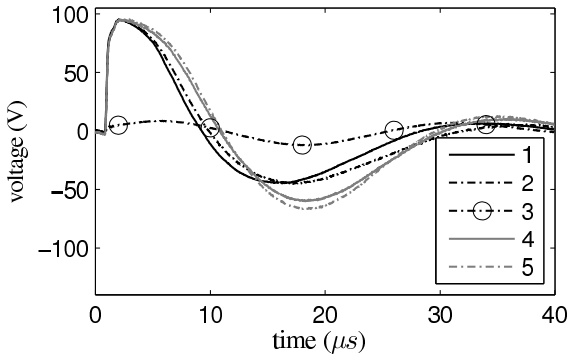

(c) Measured waveforms

Fig. 11. Calculated and measured phase voltages for different excitation modes. Calculated waveforms in (a) and (b), measured waveforms in (c). The rotor is aligned with phase A. DC bus voltage 100 V. Traces: v_a response to voltage pulse in A with B and C not connected (1), v_a response to voltage pulse in A with B and C connected (2), v_b response to voltage pulse in A with B and C connected (3), v_a response to voltage pulse in A and B with C connected (4), v_a response to voltage pulse in A, B and C (5).

In the same way, the voltage response can be calculated if test pulses are simultaneously applied in different motor phases. Two cases are considered here. In the first case, voltage pulses are simultaneously applied to phase A and B; the vector of initial voltages associated with this case is given by

$$\boldsymbol{v}(t=0) = \begin{bmatrix} v_a(t=0) \\ v_b(t=0) \\ v_c(t=0) \end{bmatrix} = \begin{bmatrix} V_{\text{dc}} \\ V_{\text{dc}} \\ 0 \end{bmatrix}. \tag{25}$$

In the second case, voltage pulses are simultaneously applied to the three phases of the machine. The vector of initial voltages associated with this case is given by

$$\boldsymbol{v}(t=0) = \begin{bmatrix} v_a(t=0) \\ v_b(t=0) \\ v_c(t=0) \end{bmatrix} = \begin{bmatrix} V_{\text{dc}} \\ V_{\text{dc}} \\ V_{\text{dc}} \end{bmatrix}. \tag{26}$$

The same procedure as described in section III can be followed. First, (25) and (26) are transformed into a virtual system, characterized by the orthogonal eigenvectors (20). Next, the response in the virtual system is transformed back to obtain the response of the phase voltages in the original system.

The voltage response of phase A to the excitation with simultaneous test pulses is shown by waveforms 4 and 5 in Fig. 11(a) and Fig. 11(b). Generally, the amplitude of the resulting waveforms is larger than in the case when only one phase is excited. This can be explained by the fact that the initial energy stored in the parasitic capacitance is larger for the case where multiple phases are excited. For an increased amount of initial energy, the subsequent resonance will oscillate with a larger amplitude.

V. Calculation versus Measurement

The different cases of voltage pulse excitation, discussed in the previous section, were experimentally applied to the switched reluctance motor. The results are shown in Fig. 11(c). A DC bus voltage of 100 V was used in the experiments. The initial voltage over the phase A winding is slightly less than 100 V, due to the saturation voltage of the two switched-on IGBTs in the converter bridge. The voltage waveforms are strongly damped due to the induced eddy currents and hysteresis losses in the magnetic core of the machine.

Comparison of the calculated waveforms of Fig. 11(b) with the measured waveforms of Fig. 11(c) shows a good correspondence. Although the eigenmode analysis is performed on an idealized system with the assumptions described in section III, it results in a good prediction of the waveforms in a

time frame of more than one half of the observed oscillation periods. The time instant t_s for the voltage measurement in Fig. 5(b) shows that this time frame is relevant for extracting rotor position information. Beyond this time frame the position resolution deteriorates due to a decreased difference between unaligned and aligned voltage samples. Moreover, the position signature between the unaligned and aligned position could not be monotonous anymore.

The discussed eigenmode analysis is a fast analytical method to predict the influence of the inductive coupling between the phases on the voltage response to test pulses. However, in some cases the method might not yield reliable results. Examples could involve large motors with small air gaps (leading to a non-negligable frequency-dependence of inductances) and having many stator poles (leading to larger ratios of mutual-to-self inductance and thus to a larger range of resonance frequencies). Another limitation of the method is that results are given for an idealized undamped system. For the analysis of large/multi-pole and/or damped systems, a nonlinear set of differential equations has to be solved, preferably by numerical methods. The advantage of the eigenmode analysis of the undamped system is that, in many cases, good qualitative predictions are made with a minimum computational effort.

VI. Conclusions

The goal of this paper is to give an insight in one aspect of the high-frequency behaviour of switched reluctance machines. At high frequencies the combination of power-electronic converter and motor phases defines a system comprising different resonant circuits, each associated with one phase of the machine. The inductive and capacitive elements in each resonant circuit are formed by a motor phase inductance and the parasitic capacitance of converter switches, power cable and phase winding. Moreover, these resonant circuits are mutually coupled due to the inductive coupling between the motor phases.

The system of mutually coupled resonant circuits has been analyzed by means of an eigenmode analysis. From this analysis, the eigenmodes and eigenfrequencies of the system were calculated.

The model of the coupled circuits has been experimentally verified. Very short test pulses were applied to a motor phase. These test pulses initiate phase voltage oscillations in all phases, which can be used to estimate the rotor position. The oscillations are a superposition of eigenmodes of the coupled system. The waveforms were calculated for the case where the test pulses are applied to a single phase and for the case where the test pulses are applied simultaneously to different phases. A good correspondence between calculated and measured waveforms was shown.

The model can be used to determine the influence of the voltage pulses, and the way they are applied, on the damped phase voltage oscillation, and thus on the rotor position estimation.

References

[1] P. Laurent, M. Gabsi, and B. Multon, "Sensorless rotor position analysis using resonant method for switched reluctance motor," in *Conference Record of the 1993 IEEE Industry Applications Society Annual Meeting.*, vol. 1, Toronto, Canada, Oct. 1993, pp. 687–694.

[2] K. R. Geldhof, A. Van den Bossche, and J. A. A. Melkebeek, "Rotor position estimation of switched reluctance motors based on damped voltage resonance," *IEEE Trans. Ind. Electron.*, submitted.

[3] K. Geldhof and A. Van den Bossche, "Resonance-based rotor position estimation in salient machines," United Kingdom Patent Request 0 813 226.8, Jul. 18, 2008.

[4] I. Husain and M. Ehsani, "Rotor position sensing in switched reluctance motor drives by measuring mutually induced voltages," *IEEE Trans. Ind. Appl.*, vol. 30, no. 3, pp. 665–672, May/Jun. 1994.

[5] K. R. Geldhof, A. Van den Bossche, and J. A. A. Melkebeek, "Influence of eddy currents on resonance-based position estimation of switched reluctance drives," in *International Conference on Electrical Machines and Systems, ICEMS 2008*, Wuhan, China, Oct. 17–20, 2008, pp. 2820–2825.

[6] H. Josephs and R. Huston, *Dynamics of mechanical systems*. Boca Raton, USA: CRC Press, 2002, pp. 450–455.

[7] M. Krishnamurthy, C. S. Edrington, A. Emadi, P. Asadi, M. Ehsani, and B. Fahimi, "Making the case for applications of switched reluctance motor technology in automotive products," *IEEE Trans. Power Electron.*, vol. 21, pp. 659–675, May 2006.

[8] Y. Liu and P. Pillay, "Improved torque performance of switched reluctance machines by reducing the mutual saturation effect," *IEEE Trans. Energy Convers.*, vol. 19, no. 2, pp. 251–257, Jun. 2004.